



Modification of BiVO₄/WO₃ composite photoelectrodes with Al₂O₃ via chemical vapor deposition for highly efficient oxidative H₂O₂ production from H₂O

Journal:	<i>Sustainable Energy & Fuels</i>
Manuscript ID	SE-ART-02-2018-000070.R1
Article Type:	Paper
Date Submitted by the Author:	06-Apr-2018
Complete List of Authors:	<p>Miyase, Yuta; National Institute of Advanced Industrial Science and Technology, Energy Technology Research Institute; Tokyo University of Science, Department of Pure and Applied Chemistry Takasugi, Soichi; National Institute of Advanced Industrial Science and Technology, Research Center for Photovoltaics Iguchi, Shoji; National Institute of Advanced Industrial Science and Technology, Research Center for Photovoltaics Miseki, Yugo; National Institute of Advanced Industrial Science and Technology, Gunji, Takahiro; Tokyo University of Science, Department of Pure and Applied Chemistry SASAKI, KOTARO; Brookhaven National Laboratory, Chemistry Department Fujita, Etsuko; Brookhaven National Laboratory, Chemistry Department Sayama, Kazuhiro; National Institute of Advanced Industrial Science and Technology, Energy Technology Research Institute; Tokyo University of Science</p>

Modification of BiVO₄/WO₃ composite photoelectrodes with Al₂O₃ via chemical vapor deposition for highly efficient oxidative H₂O₂ production from H₂O

Yuta Miyase^{a,b}, Soichi Takasugi^a, Shoji Iguchi^a, Yugo Miseki^a, Takahiro Gunji^{a,b}, Kotaro Sasaki^c, Etsuko Fujita^c and Kazuhiro Sayama^{*a,b}

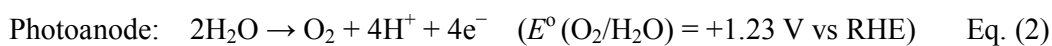
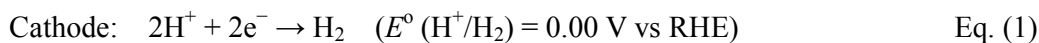
- a. Research Center for Photovoltaics, National Institute of Advance Industrial Science and Technology, Central 5, 1-1-1 Higashi, Tsukuba, Ibaraki 3058565, Japan. E-mail: k.sayama@aist.go.jp
- b. Department of Pure and Applied Chemistry, Tokyo University of Science, 2641 Yamasaki, Noda, Chiba 2788514, Japan.
- c. Chemistry Division, Brookhaven National Laboratory, Upton, New York, 11973-5000, USA.

Abstract

The modification of a BiVO₄/WO₃ photoelectrode with Al₂O₃ by a chemical vapor deposition (CVD) method significantly improved the Faradaic efficiency for H₂O₂ production (FE(H₂O₂)) in the photoelectrochemical oxidation of H₂O. The Faradaic efficiency after passing 0.9 C (after the photoirradiation for 15 min using simulated solar light), was 80% using a 2.0 M KHCO₃ aqueous solution as an electrolyte. An initial FE(H₂O₂) (< 0.02 C) was almost 100% on the Al₂O₃/BiVO₄/WO₃ photoelectrode. The thin Al₂O₃ layer prevents the oxidative decomposition of the produced H₂O₂ into O₂. The applied bias photon to current efficiency (ABPE) was 2.57% based on H₂O₂ and O₂ production on the photoanode and H₂ production on a Pt cathode. Solar light driven simultaneous H₂O₂ production at the anode for H₂O oxidation and the cathode for O₂ reduction were also achieved by combining a noble-metal-free biomass-derived carbon cathode without applying any external bias.

Introduction

Since the Honda-Fujishima effect has been reported, water-splitting into H₂ and O₂ using a photoelectrochemical cell has been identified as a promising technique for an effective solar energy conversion and storage system.¹⁻³ Such systems enable water-splitting at a lower external bias than the thermodynamic value ($\Delta E^0 = 1.23$ V) by utilizing solar energy effectively. The water splitting into H₂ and O₂ on the cathode and photoanode is presented in Eqs. (1) - (3), respectively.



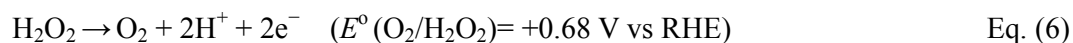
It is favorable to utilize metal oxide films such as WO₃,⁴⁻⁶ BiVO₄,^{7,8} and Fe₂O₃⁹ in photoelectrochemical reactions, having absorption in the visible light region. In particular, BiVO₄ is widely known as one of the most promising metal oxide materials for H₂O oxidation. It is composed of inexpensive metals, and absorbs a wide range of visible light (~520 nm) corresponding to the narrow band gap (*ca.* 2.4 eV).¹⁰ The oxidation products of H₂O such as O₂ have been paid little attention in most photoelectrochemical water-splitting system, while reduction products such as H₂ have been regarded as new clean fuels.¹¹ On the other hand, some researchers reported oxidative production of high value-added oxidants such as H₂O₂,¹²⁻¹⁶ S₂O₈²⁻,^{18,19} ClO⁻,²⁰ etc. on the photoanode with simultaneous H₂ production on the cathode. Additionally, it has been revealed that 2-electron oxidation of H₂O to H₂O₂ (Eq. (4)) might be concurrent with 4-electron oxidation to O₂.²¹



H₂O₂ has attracted considerable attention as a versatile and clean redox reagent for selective organic conversion, environmental purification, bleaching, cleaning agents, and an energy source for H₂O₂ fuel cells.²²⁻²⁴ Therefore, the development of water-splitting systems for H₂ and H₂O₂ production (Eq. (5)) would enable us to broaden the use of photoelectrode systems in various fields, while conventional water-splitting systems into H₂ and O₂ (Eq. (3)) do not make good use of the photo-induced oxidation power.



A small amount of H₂O₂ was sometimes detected in photocatalytic or photoelectrochemical H₂O oxidation, indicating that H₂O₂ can be an intermediate species of O₂ production from H₂O via 4-electron oxidation. Inevitable oxidative decomposition of the produced H₂O₂ may disable the system for oxidative production and accumulation of H₂O₂, that is, the produced H₂O₂ might be easily decomposed into O₂ by generated holes (h⁺) in accordance with Eq. (6). Moreover, the H₂O₂ production from H₂O via a 2-electron process (Eq. (4)) should compete with the O₂ production from H₂O via a 4-electron process (Eq. (2)), which is more preferential than H₂O₂ production in consideration of their redox potentials. Hence, the development of tailor-made photoanodes that can prevent the oxidative decomposition of the produced H₂O₂ into O₂, should accelerate the photoelectrochemical H₂O₂ production and accumulation from H₂O.

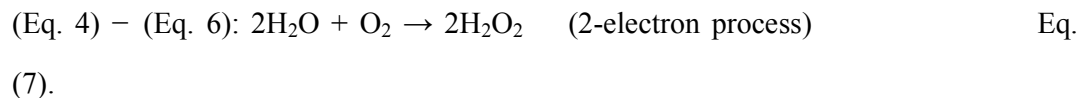


In our previous work, we found the unique phenomenon that the presence of the

bicarbonate anion (HCO_3^-) in the electrolyte solution enabled us to achieve a significant improvement in the Faradaic efficiency for oxidative H_2O_2 generation ($\text{FE}(\text{H}_2\text{O}_2)$) in the photoelectrochemical reaction using the $\text{BiVO}_4/\text{WO}_3$ photoelectrode.¹³⁻¹⁵ It was expected that the percarbonate/bicarbonate couple played an important role in effective H_2O_2 production and accumulation.²⁵ Our original $\text{BiVO}_4/\text{WO}_3$ multilayer photoelectrode is composed of BiVO_4 and WO_3 , which worked as a photocatalyst layer (light absorption layer) and an effective electron transporting layer, respectively.^{26,27} It is also reported that the BiVO_4 surface was suitable for H_2O_2 production in bicarbonate solution under dark conditions.^{16,28} The value of the applied bias photon to current efficiency (ABPE) under simulated solar light irradiation (1 Sun: AM-1.5, 100 mW cm^{-2}) was 2.2% by considering production of H_2O_2 , O_2 and H_2 . Moreover, we have recently reported that the $\text{FE}(\text{H}_2\text{O}_2)$ was drastically improved from 54% to 79% by surface modification of the $\text{BiVO}_4/\text{WO}_3$ photoelectrode with a porous and thick Al_2O_3 layer prepared via a metal organic decomposition (MOD) method (hereinafter, $\text{Al}_2\text{O}_3(\text{MOD})$).¹⁵ However, the modification obviously deteriorated the photocurrent-potential property and caused a decrease in the ABPE value from 2.2% to 1.5%. In the present study, we investigate the modification of the $\text{BiVO}_4/\text{WO}_3$ photoelectrode with a thin Al_2O_3 layer produced by the chemical vapor deposition method ($\text{Al}_2\text{O}_3(\text{CVDn})$ where n = number of CVD cycles) with the aim of high $\text{FE}(\text{H}_2\text{O}_2)$ and ABPE values.

When BiVO_4 was used as a photoanode, it was necessary to apply an external bias for inducing H_2 production on the counter electrode because the potential of the bottom of the conduction band (ca. +0.02 V vs RHE)²⁹ was more positive than the standard potential for H_2 production (H^+/H_2 : 0.00 V vs RHE). On the other hand, the standard potential for reductive H_2O_2 production from O_2 ($\text{O}_2/\text{H}_2\text{O}_2$: +0.68 V vs RHE) was more positive than that for H_2 production and the bottom of its conduction band. Therefore, a BiVO_4 photoanode may cause H_2O_2 production on the counter electrode without

applying an external bias. In fact, we reported that a photoelectrochemical cell composed of a Au cathode and the BiVO₄/WO₃ photoanode achieved H₂O₂ production without applying any external bias under simulated solar light irradiation, as shown in Eq. (7) via the 2-electron process.¹⁴



However, it is preferable not to use expensive noble metals such as Au. Recently, we have reported that carbon-paper cathodes composed of a biomass-derived W- or Mo-carbide/nitride composite on carbon paper showed high performance for electrochemical H₂ evolution at pH1.^{30,31} Here we investigate the activity of the reductive H₂O₂ production from O₂ in a bicarbonate solution using these biomass-derived electrocatalysts over carbon-based cathodes. Moreover, a new photoelectrochemical cell composed of a Al₂O₃(CVD5)/BiVO₄/WO₃ photoanode and W-based cathode successfully produced solar light driven H₂O₂ on both electrodes without applying any external bias or using noble metals.

Experimental Section

Preparation of electrode

1. BiVO₄/WO₃ and Al₂O₃/BiVO₄/WO₃ photoelectrodes

The BiVO₄/WO₃ photoelectrode was prepared on a conductive glass substrate (FTO: F-doped SnO₂) by the spin-coating method as we have previously reported.¹³ The precursor of the WO₃ layer was loaded by spin-coating (1000 rpm, 15 s, 200 μL per 12 cm²) on FTO and then calcined at 773 K for 30 min. The spin-coating of the WO₃ layer was repeated twice using *N,N*-dimethylformamide (DMF) solutions of tungsten hexachloride (WCl₆) adjusted to 504 mM and 252 mM, respectively. The BiVO₄ layer was also fabricated by spin-coating (500 rpm, 15 s, 400 μL per 12 cm²) on the WO₃ layer and calcined at 773 K for 30 min. The BiVO₄ precursor solution, adjusted to 100 mM, was prepared by dissolving bismuth oxide (BiO_{1.5}) solution (Symmetrix Co., USA), and a vanadium oxide (VO_{2.5}) solution (Symmetrix Co., USA) in butyl acetate with a Bi/V molar ratio of 1.0. A 10wt% butyl acetate solution of ethyl cellulose was added to the BiVO₄ solution as a thickening agent with a (BiVO₄ solution) / (ethyl cellulose solution) volume ratio of 1.5. The surface area of photoanode was changed in order to evaluate produced H₂O₂ accurately and to minimize the effect of successive H₂O₂ decomposition.

The BiVO₄/WO₃ photoelectrode was modified with Al₂O₃ by two methods: a conventional wet process using the MOD method¹⁵ and a dry process based on chemical vapor deposition (CVD). The surface modification by CVD was performed using SAL3000Plus (SUGA Co., Japan). The temperature of the CVD unit was kept stable at 423 K, and vapor trimethylaluminum (TMA) and H₂O were alternately introduced into the heated sample chamber at 30 s intervals per cycle. In the case of the MOD method, the optimized conditions in the previous work were used.¹⁵ The BiVO₄/WO₃ photoelectrode modified with Al₂O₃ using the CVD method and the MOD method are denoted as the Al₂O₃(CVDn)/BiVO₄/WO₃ (where, n = number of CVD cycles) and the

$\text{Al}_2\text{O}_3(\text{MOD})/\text{BiVO}_4/\text{WO}_3$ photoelectrode, respectively. The prepared photoelectrodes were characterized by X-ray fluorescence (XRF, Rigaku, ZSX mini, measured in vacuum with a wavelength dispersive spectrometer, analysis area: 3cm^2) with Pd-K or -L radiation, X-ray photoelectron spectroscopy (XPS, ULVAC, PHI) with Al- K_α radiation, and scanning electron microscopy (SEM, HITACHI High-Technologies Co. S-4800), X-ray diffraction (XRD, PANalytical, IC Vario) with Cu- K_α , and UV-Vis spectroscopy (JASCO, V570).

2. Biomass-derived carbon cathode (WSoy/GnP-CP, MoSoy-CP, CB-CP)

Biomass-derived W- and Mo-based electrocatalysts (WSoy and MoSoy) were synthesized following the previous reports.^{30,31} WSoy/GnP, tungsten carbide/nitride composite supported on graphene nanoplatelets (GnP), was prepared by a sintering process. A mixture of 100 mg of GnP (XG Sciences C-750) and 100 mg of ground soybean (Whole Food Market Inc., USA) was added to a 0.64 mM aqueous solution (50 mL) of ammonium tungstate tetra hydrate (Sigma-Aldrich Co., USA). The suspension was thoroughly dispersed by ultrasonication for 30 min and dried at 353 K overnight under ambient pressure in a heating oven. The dried powder was calcined at 1123 K in an Ar atmosphere for 2 h in a quartz tube furnace. MoSoy was synthesized by a similar method using mixtures of 100 mg of ammonium molybdate tetrahydrate (Sigma-Aldrich Co., USA) and 100 mg of soybean, and sintering at 1073 K for 2 h. A mixture of 1.5 mg (standard amount) of the electrocatalyst (WSoy/GnP, MoSoy, or carbon black (CB, VULCAN XC-72, CABOT Co., USA)) and 0.75 mg of a 20wt% Nafion solution (Sigma-Aldrich Co., USA) was dispersed in 0.5 mL ethanol and loaded on one side of water-repellent treated carbon paper (CP, 1.0 cm^2 , TORAY, TGP-H-090).

Photoelectrochemical reaction for H_2O_2 production and accumulation

H₂O₂ production was performed using a two-chamber cell with a Nafion membrane (Nafion NRE-212, Sigma-Aldrich Co., USA) separating the Al₂O₃-modified BiVO₄/WO₃ photoanode (6 cm²) and a Pt-mesh electrode as a cathode and a quasi-reference electrode. An aqueous solution of KHCO₃ was utilized as an electrolyte solution (35 mL each for the anode and cathode chambers), and CO₂ gas was continuously bubbled into the solution to keep the pH value at 7.0 – 7.8 during the reaction. The solution was cooled with an ice bath (273 - 278 K) to prevent the thermal decomposition of the produced H₂O₂. A solar simulator (XES-151S, SAN-EI ELECTRIC Co.) calibrated to AM 1.5 G (1 SUN, 100mW cm⁻², JIS-A-class) was used as the light source. The anodic photocurrent was kept at 1.0 mA by using an electrochemical analyzer (ALS660E, BAS. Inc.). The amount of H₂O₂ produced was quantified by colorimetry using 0.1 M FeCl₂ in 1.0 M HCl aqueous solution, as we reported previously.¹³ In addition, produced O₂ in the gas and liquid phase was measured with an O₂ meter (PyroScience, Firesting O₂) in the sealed reaction cell. The Faradaic efficiency for H₂O₂ production (FE(H₂O₂)) was calculated in accordance with Eq. (8).

$$\text{FE}(\text{H}_2\text{O}_2) = [\text{amount of produced H}_2\text{O}_2 (\mu\text{mol})] \times 100 / [\text{passed electrons } (\mu\text{mol}) / 2]$$

Eq. (8)

Photoelectrochemical properties and calculation of applied bias photon-to-current conversion efficiency (ABPE)

The current-potential (I-V) curves of the fabricated photoelectrodes were measured using a three-electrode system composed of a photoanode (irradiation area: 0.28 cm², with white board behind photoelectrode), a Pt wire cathode, and a Ag/AgCl reference electrode. The applied bias photon-to-current conversion efficiency (ABPE) for the H₂O₂ and O₂ production on the photoanode and H₂ production on the cathode

was calculated using the photocurrent-potential properties and Faradaic efficiencies of H_2O_2 and O_2 after passing 0.9 C, as shown in Eq. (9),^{32,33}

$$\begin{aligned} \text{ABPE}(\%) = & [J_{\text{opt}} \times (1.77 \text{ V} - E_{\text{opt}}) / Int] \times \text{FE}(\text{H}_2\text{O}_2) \\ & + [J_{\text{opt}} \times (1.23 \text{ V} - E_{\text{opt}}) / Int] \times \text{FE}(\text{O}_2) \end{aligned} \quad \text{Eq. (9)}$$

where,

J_{opt} is the photocurrent density at E_{opt} ,

E_{opt} is the applied external voltage at optimal conditions between working and counter electrodes,

Int is the intensity of incident simulated solar light (100 mW cm^{-2}),

$\text{FE}(\text{H}_2\text{O}_2)$ and $\text{FE}(\text{O}_2)$ are the Faradaic efficiencies of H_2O_2 and O_2 , respectively.

The standard potentials of H^+/H_2 , $\text{O}_2/\text{H}_2\text{O}$ and $\text{H}_2\text{O}_2/\text{H}_2\text{O}$ are also applied to this equation.

Investigation of reductive H_2O_2 production and accumulation

The current-potential (I-V) curves for H_2O_2 production using various cathodes were measured by an electrochemical analyzer (BAS Inc., ALS660E) using a three-electrode system composed of a cathode electrode, a Pt-mesh anode and a Ag/AgCl reference electrode in a 2.0 M KHCO_3 aqueous solution (35 mL each for the anode and cathode chambers). H_2O_2 production was performed using a three-electrode system in a two-chamber cell separated by a Nafion membrane between the cathode chamber containing a cathode electrode (standard amount of catalyst loading: 1.5 mg cm^{-2} ; area: 1 cm^2) and a Ag/AgCl reference electrode and the anode chamber containing a Pt-mesh counter electrode. An aqueous solution of 2.0 M KHCO_3 with O_2 bubbling at a flow rate of 50 mL min^{-1} was utilized as an electrolyte (pH 8.6), and the solution was cooled with an ice bath (273 – 278 K) to prevent the thermal decomposition of the produced H_2O_2 .

A stable external bias of +0.5 V (vs RHE) was applied to the cathode during the reaction.

Simultaneous H₂O₂ production on both the photoanode and cathode without external bias

The simultaneous production of H₂O₂ from H₂O oxidation at the photoanode and O₂ reduction at the cathode was performed without applying any external bias using a two-electrode system composed of a Al₂O₃(CVD5)/BiVO₄/WO₃ photoanode (12 cm²) and a WSoy/GnP-CP cathode (catalyst loading: 1.5 mg cm⁻², area: 12 cm²). A 2.0 M KHCO₃ aqueous solution was used as an electrolyte (35 mL each for the anode and cathode chamber), and CO₂ and O₂ gases were bubbled into the anode and cathode chambers of the two-component cell, respectively. It is known that the electrochemical reaction should be accelerated when the pH value of the anolyte solution is higher than that of the catholyte solution.³⁴ In the case of the present study, the difference in pH value between them (anolyte: 7.9, catholyte: 8.6) will be a little disadvantageous for simultaneous H₂O₂ production on both the photoanode and cathode without external bias. The solution was cooled with an ice bath (273-278 K) to prevent the thermal decomposition of the produced H₂O₂. A solar simulator calibrated to AM 1.5G (1SUN, 100 mW cm⁻²) was used as the light source.

Result and Discussion

H₂O₂ production from H₂O on BiVO₄/WO₃ photoelectrode modified with Al₂O₃

Figure 1 shows the concentration of H₂O₂ produced in a 0.5 M KHCO₃ aqueous solution during the photoelectrochemical H₂O oxidation over a Al₂O₃(CVDn)/BiVO₄/WO₃ (n = 0 – 10) photoanode under simulated solar light irradiation. The amount of H₂O₂ produced improved upon an increasing number of CVD cycles, and the H₂O₂ concentration reached 88 μM (FE(H₂O₂) = 67%) on the Al₂O₃(CVD5)/BiVO₄/WO₃ photoelectrode after passing 0.9 C, while a bare photoelectrode (i.e., no Al₂O₃ coating) produced 55 μM (FE(H₂O₂) = 41%). The amount of Al₂O₃ loaded on the BiVO₄/WO₃ photoelectrode obviously increased with the number of CVD cycles. These results indicate that the modification of the BiVO₄/WO₃ photoelectrode with Al₂O₃ might change its surface properties corresponding to photoelectrochemical H₂O₂ production. The concentration of bicarbonate ions (HCO₃⁻) in the electrolyte solution affected the H₂O₂ production, and H₂O₂ was produced at a FE(H₂O₂) of 80% over the Al₂O₃(CVD5)/BiVO₄/WO₃ photoelectrode when 2.0 M KHCO₃ aqueous solution was used as the electrolyte solution (Figure S1). The amount of H₂O₂ produced over the Al₂O₃(CVD5)/BiVO₄/WO₃ photoelectrode, which was the best CVD cycle, was commensurate with the case of the Al₂O₃(MOD)/BiVO₄/WO₃ photoelectrode reported in our previous paper (Figure S2(A)).¹⁵ The applied external bias on the Al₂O₃(CVD5)/BiVO₄/WO₃ was same as BiVO₄/WO₃ photoelectrode (Figure S2(B)). Moreover, the effect of Al₂O₃ modification with the CVD method remained even in prolonged reaction to 50 C (Figure S3). The FE values of H₂O₂ production on photoelectrodes were not influenced by the magnitude of the applied bias (Figure S4). Figure 2 shows the I-V curves of each photoelectrode: (a) Al₂O₃(CVD5)/BiVO₄/WO₃, (b) Al₂O₃(MOD)/BiVO₄/WO₃, and (c) bare BiVO₄/WO₃ measured in 2.0 M KHCO₃ aqueous solution. The photoelectrode modified with Al₂O₃(MOD) exhibited lower photocurrent density than the bare BiVO₄/WO₃ photoelectrode, indicating that thick

Al₂O₃ layers fabricated by the MOD method might disrupt the electrical contact between the BiVO₄ and the electrolyte.¹⁵ Contrary to this, the Al₂O₃ layer loaded by the CVD method did not influence the photocurrent density. Accordingly, modification of BiVO₄/WO₃ with Al₂O₃(CVD) enabled superior Faradaic efficiency for H₂O₂ production while maintaining good photocurrent-potential properties.

The distinctive peaks corresponding to BiVO₄, WO₃, and SnO₂ were clearly observed in XRD patterns (Figure S5). The BiVO₄/WO₃ photoelectrode modified by both the MOD method and the CVD method did not exhibit diffraction peaks corresponding to Al₂O₃, indicating that the prepared Al₂O₃ layer on the surface of the photoelectrode should be amorphous-like in structure. XRF analysis revealed that the amount of modified Al₂O₃ on the photoelectrode through 5 CVD cycles was $2.2 \times 10^{-2} \text{ mg cm}^{-2}$ (Figure 1), and it was less than that on the photoelectrode modified with the MOD method ($5.5 \times 10^{-2} \text{ mg cm}^{-2}$). The top-view and side-view of the SEM images of the bare and Al₂O₃-modified photoelectrodes are shown in Figures 3(A) and 3(B), respectively. The 100 – 150 nm thickness of BiVO₄ worm-like particle layer (Figure 3(Aa)) was loaded on the 100 – 120 nm thickness of the WO₃ layer, which has rather a smooth surface (Figure 3(Ad)) on the FTO substrate. In the case of MOD method, the Al₂O₃ layer almost thoroughly covered the BiVO₄/WO₃ photoelectrode (Figures 3(Ab) and (Bb)), whereas a mesoporous structure corresponding to pinholes or cracks were partially observed (Figure 3(Ab)). It is speculated that H₂O₂ was produced on the surface of BiVO₄ layers through the mesoporous structure of Al₂O₃.¹⁵ On the other hand, in the case of the CVD method, the worm-like shape of BiVO₄ particles was clearly observed despite the presence of Al₂O₃, similar to the bare photoelectrode (Figures 3(Aa) and 3(Ac)). The location of Al₂O₃ loaded by the CVD method could not be identified by SEM images. The apparent surface elemental ratio of each photoelectrode, calculated from XPS spectra, are shown in Figure 4. Both BiVO₄ and WO₃ were covered with Al₂O₃ thoroughly by the MOD method (Figure 4(b)). On the other hand, a

tiny part of BiVO₄ was covered with Al₂O₃ introduced by the CVD method, while the majority of WO₃ and SnO₂ were covered by Al₂O₃ (Figure 4(c)). It is speculated that the precursor of Al₂O₃ (precursor gas: TMA) was more easily absorbed or hydrolyzed on the WO₃ and SnO₂ layers compared to BiVO₄ layer. As shown in Figure S6, the surface elemental ratio of WO₃ in the Al₂O₃(CVD)/BiVO₄/WO₃ photoelectrode was significantly decreased with the increasing number of CVD cycles, whereas that of BiVO₄ was not decreased within 5 cycles of CVD. It can be estimated that Al₂O₃ was deposited on the exposed part of the WO₃ layer preferentially by the CVD method. FE(H₂O₂) was clearly improved by Al₂O₃(CVD) modification in accordance with the decrease in the exposed WO₃ ratio. When the amount of Al₂O₃ loaded by the MOD method (XRF based: 2.0×10^{-2} mg cm⁻², Figure 4(d)) was the same as in the CVD method (5cycles, 2.2×10^{-2} mg cm⁻²), the surface of BiVO₄ was thoroughly covered by Al₂O₃ introduced by the MOD method. The value of ABPE, indicating the conversion efficiency of the solar light energy to chemical energy, was decreased using the Al₂O₃(MOD)/BiVO₄/WO₃ photoelectrode in comparison with the bare photoelectrode (Figure 5), because the photocurrent-potential property was significantly deteriorated by Al₂O₃ modification with the MOD method, which seems to completely cover the BiVO₄ layer (Figure 2). On the other hand, we achieved the highest ABPE value of 2.57% by using the Al₂O₃(CVD5)/BiVO₄/WO₃ photoelectrode, which enabled high FE(H₂O₂) and superior photocurrent-potential properties simultaneously.

Figure 6 exhibits the amount of H₂O₂ produced in the photoelectrochemical H₂O oxidation using three kinds of fabricated photoelectrodes. It is noteworthy that the initial FE(H₂O₂) at less than 0.02 C was close to 100% for all photoelectrodes regardless of the Al₂O₃ modification, on the other hand, The FE(H₂O₂) decreased with time due to oxidative decomposition of H₂O₂ into O₂. The faradic efficiency of O₂ production (FE(O₂)) as shown in Figure S7, and sum of FE(H₂O₂) and FE(O₂) was found to be nearly 100% under the reaction condition. (Figure S7). The decrease in FE(H₂O₂) for

the $\text{Al}_2\text{O}_3(\text{CVD})$ - and $\text{Al}_2\text{O}_3(\text{MOD})$ -modified photoelectrodes was much slower than that for the bare photoelectrode, indicating that an Al_2O_3 layer loaded on the photoelectrode might suppress the decomposition of the produced H_2O_2 into O_2 . Figures S8(a) - (c) show the decomposition profiles of H_2O_2 in the presence of photoelectrodes without applying an external bias. H_2O_2 was barely decomposed in the case of the dark condition for 60 min. However, H_2O_2 was drastically decomposed under simulated solar light irradiation for all photoelectrodes, indicating that photo-generated carriers (electron and hole) on the photoelectrodes caused the decomposition of H_2O_2 . The decomposition rates of H_2O_2 were obviously suppressed by modification of photoelectrodes with the CVD (Figure S8(a)) and MOD (Figure S8(b)) methods. The decomposition rate over a BiVO_4 photoelectrode without WO_3 (Figure S8(d)) was much slower than that over a WO_3 photoelectrode (Figure S8(e)) under simulated solar light irradiation, whereas amounts of photo-generated carriers for WO_3 was much smaller than those for BiVO_4 considering the light harvesting efficiencies (LHE) in Figure S9. We also confirmed that modification of WO_3 with Al_2O_3 by the CVD method clearly inhibits the H_2O_2 decomposition under the same conditions as Figure S8. These results suggested that H_2O_2 was easily decomposed on WO_3 , and the modification of the $\text{BiVO}_4/\text{WO}_3$ photoelectrode with Al_2O_3 effectively suppressed the decomposition of the produced H_2O_2 by blocking contact to the WO_3 as shown in Figure S10. Moreover, an Al_2O_3 layer fabricated by the MOD method on the photoelectrode, which thoroughly covers the BiVO_4 layer, caused the deterioration of the photocurrent-potential property (Figure 2). On the other hand, Al_2O_3 loading by the CVD method, masking WO_3 and SnO_2 preferentially, achieves an improvement in the $\text{FE}(\text{H}_2\text{O}_2)$ without degrading the photocurrent-potential property. Accordingly, high ABPE values were obtained by the present study.

Reductive H₂O₂ production from O₂ on cathode

Figure 7 shows the cathodic current density for O₂ reduction on various cathodes such as MoSoy-CP, WSoy/GnP-CP, CB-CP, Au wire, and bare CP in 2.0 M KHCO₃ aqueous solution. The cathodic current corresponding to O₂ reduction over these fabricated cathodes were much higher than that over the Au cathode. Moreover, the onset potential of MoSoy-CP and WSoy/GnP-CP were more positive than those of CB-CP and Au. Among them, the WSoy/GnP-CP composite cathode showed the highest cathodic current density for the electrochemical reduction of O₂ in an aqueous KHCO₃ electrolyte solution. Table 1 shows the total current density for O₂ reduction, FE(H₂O₂) after 1.0 C of electric charge was passed, and current density for H₂O₂ production in the electrochemical reactions at +0.5 V (vs RHE) using various cathodes. CB and Au showed high FE(H₂O₂), while the total current density and the current density for H₂O₂ production of both cathodes were low. On the other hand, WSoy/GnP showed large current density and relatively high FE(H₂O₂) of 39% (the rest might be H₂O production from O₂.) simultaneously, indicating that the CP cathode with WSoy/GnP showed the highest H₂O₂ production performance (cathodic current density for H₂O₂ production: -1.1 mA cm^{-2}). Moreover, this catalyst was stable under these reaction condition. Figure S11 shows the comparison of the I-V curve and the FE(H₂O₂) on the WSoy/GnP loaded cathode before / after 100 cycles of CV measurement operated under the same conditions as Figure 7. Both I-V curve and FE(H₂O₂) were unchanged after 100 cycles of CV measurement. It is noteworthy that these biomass-derived electrocatalysts reported for H₂ production could be utilized also for H₂O₂ production from O₂.

Finally, we have demonstrated H₂O₂ production with the combination of the WSoy/GnP-CP cathode (loading: 1.5 mg cm^{-2} , 12 cm^2) and the Al₂O₃(CVD5)/BiVO₄/WO₃ photoelectrode (12 cm^2) under simulated solar light irradiation in 2.0 M KHCO₃ aqueous solution (Figures 8(A) and 8(B)). The open circuit voltage was $\sim 0.30 \text{ V}$. Notably, approximately 0.7 mA of the photocurrent was observed

without applying an external bias. H_2O_2 was produced on the cathode and the photoanode with FE(H_2O_2) of 44% and 60%, respectively, after 1.8 C of electric charge was passed. Accordingly, a new photoelectrochemical cell was successfully developed by using the Al_2O_3 -modified $\text{BiVO}_4/\text{WO}_3$ photoelectrode and the biomass-derived carbon cathode, which enabled us to achieve direct conversion of solar light into chemical energy (H_2O_2 , Eq. (7)) without applying an external bias.

Summary

The modification of $\text{BiVO}_4/\text{WO}_3$ photoelectrodes with Al_2O_3 using the chemical vapor deposition (CVD) method exhibited superior Faradaic efficiency for H_2O_2 production while maintaining favorable photocurrent-potential properties, where we achieved the highest ABPE value of 2.57% by using the $\text{Al}_2\text{O}_3(\text{CVD5})/\text{BiVO}_4/\text{WO}_3$ photoelectrode among photoelectrodes we investigated. In the case of the metal organic decomposition (MOD) method, an Al_2O_3 layer fabricated on the photoelectrode thoroughly covered the BiVO_4 layer, causing the deterioration of the photocurrent-potential property. On the other hand, with the CVD method, the Al_2O_3 layer fabricated on the photoelectrode, masking WO_3 and SnO_2 preferentially, suppressed the decomposition of produced H_2O_2 on WO_3 without degrading the photocurrent-potential property. Furthermore, we discovered that the CP cathode with a biomass-derived W-based electrocatalyst (WSoy/GnP-CP) exhibited superior activity for the reductive H_2O_2 production from O_2 over an Au cathode. As a consequence, a newly developed photoelectrode cell, composed of a $\text{Al}_2\text{O}_3(\text{CVD})/\text{BiVO}_4/\text{WO}_3$ photoanode and a biomass-derived carbon cathode, enables us to achieve simultaneous production of H_2O_2 on both photoanode and cathode without applying external bias and employing a noble-metal.

Acknowledgements

We thank Dr. Wei-Fu Chen and Dr. Fanke Meng for preparation of MoSoy and WSoy/GnP, respectively, and Dr. James Muckerman for a careful reading of the manuscript. The present work was partially supported by the International Joint Research Program for Innovative Energy Technology. The work at BNL was carried out with support from the U.S. Department of Energy, Office of Science, Division of Chemical Sciences, Geosciences & Biosciences, Office of Basic Energy Sciences under contract DE-SC0012704.

Table

Table 1 Total current density of various cathodes at +0.5 V (vs RHE), FE(H₂O₂) after 1.0 C of the electric charge was passed, and the calculated current density for H₂O₂ production (total current density × FE(H₂O₂)) in the electrochemical O₂ reduction.^a

Cathode material	Total current density / mA cm⁻²	FE(H₂O₂) at 1C (%)	Current density for H₂O₂ production / mA cm⁻²
Bare CP	5.4×10^{-4}	–	–
Au coil	-4.5×10^{-2}	57	-2.5×10^{-2}
CB	-4.5×10^{-1}	83	-3.7×10^{-1}
MoSoy	-1.5	19	-2.9×10^{-1}
WSoy/GnP	-2.9	39	-1.1

^a Measurement condition: three-electrode cell with a Pt wire as a counter electrode, various cathodes as working electrodes and a Ag/AgCl reference electrode were used with a 2.0 M KHCO₃ aqueous solution under O₂ bubbling.

Figures

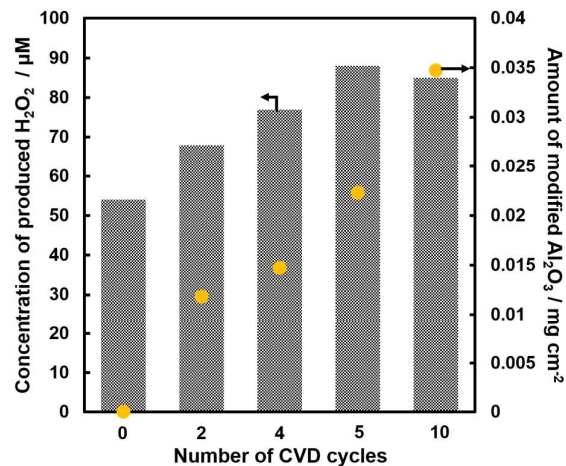


Figure 1. Concentration of H₂O₂ produced after 0.9 C of electric charge was passed (left) and the amount of loaded Al₂O₃ measured by XRF (right). Two-electrode photoelectrochemical cell with an Al₂O₃(CVD)/BiVO₄/WO₃ photoanode (6 cm²) and a Pt wire as a cathode electrode was used in a 0.5 M KHCO₃ aqueous solution under CO₂ bubbling and simulated solar irradiation by controlling the stable current of 1.0 mA.

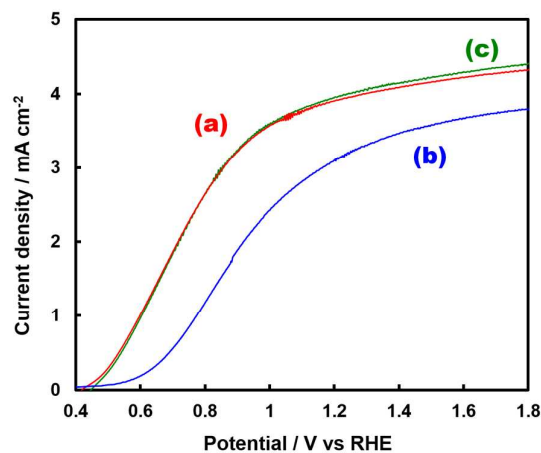
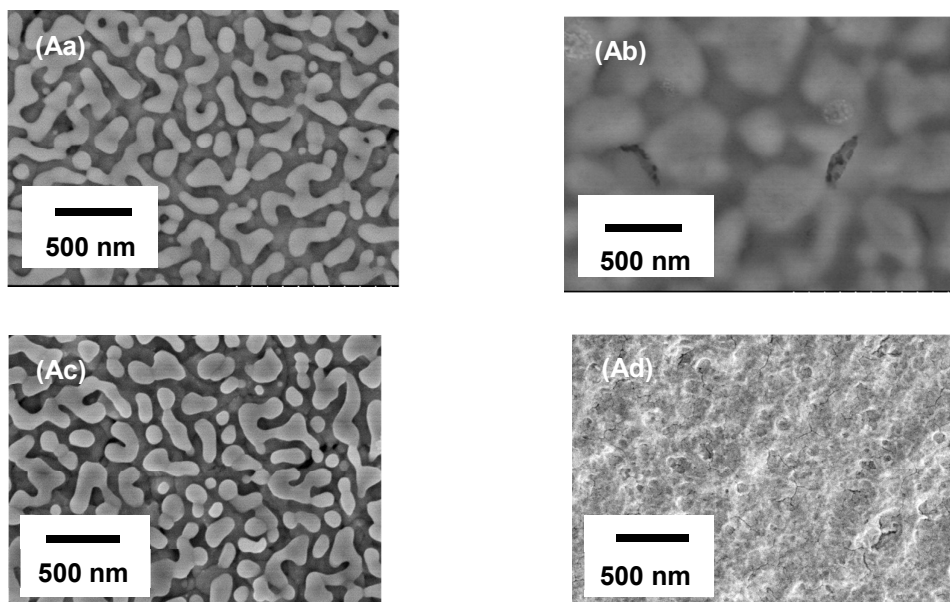


Figure 2. Current density of fabricated photoanodes (0.28 cm²): (a) Al₂O₃(CVD5)/BiVO₄/WO₃, (b) Al₂O₃(MOD)/BiVO₄/WO₃, and (c) BiVO₄/WO₃. Three-electrode cell with various photoelectrodes (a - c), a Pt wire as a cathode and an Ag/AgCl reference electrode are used in a 2.0 M KHCO₃ aqueous solution under CO₂ bubbling and simulated solar irradiation.

(A) Top-view



(B) Side-view

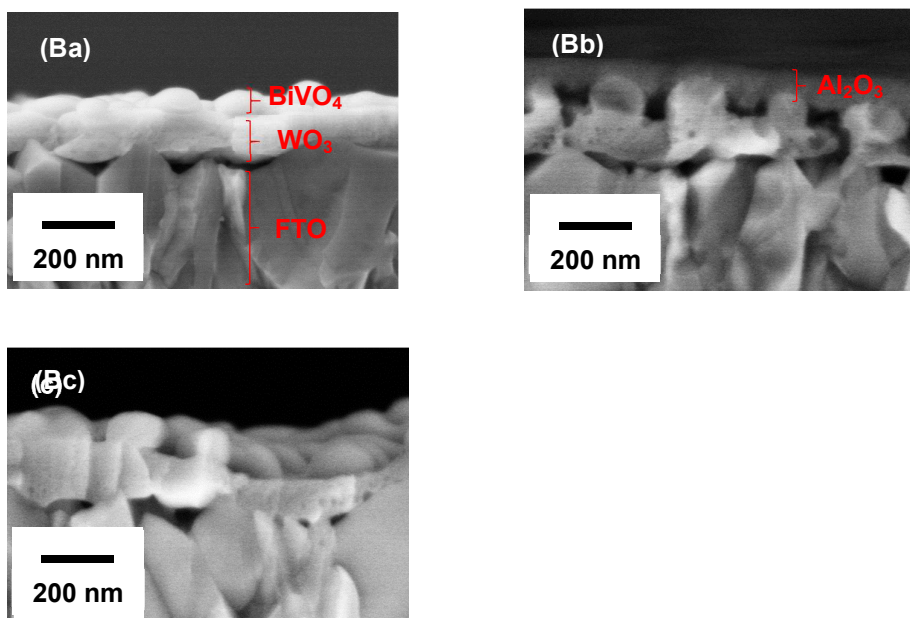


Figure 3. SEM images of top-views (A) and side-views (B) of fabricated photoelectrodes: (a) BiVO₄/WO₃, (b) Al₂O₃(MOD)/BiVO₄/WO₃, (c) Al₂O₃(CVD5)/BiVO₄/WO₃, and (d) WO₃ photoelectrode.

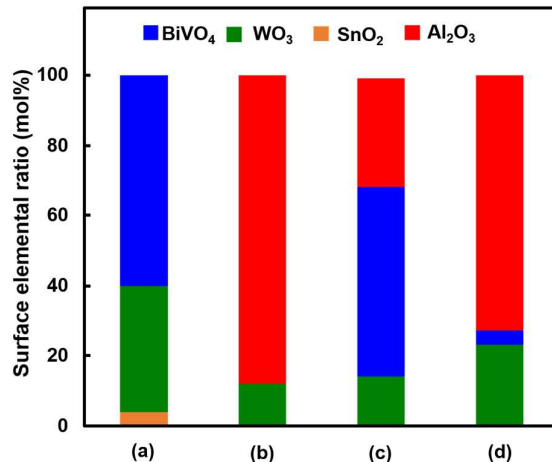


Figure 4. Surface elemental ratio of fabricated photoelectrodes: (a) BiVO₄/WO₃, (b) Al₂O₃(MOD)/BiVO₄/WO₃ (Al₂O₃: 5.5×10^{-2} mg cm⁻²), (c) Al₂O₃(CVD5)/BiVO₄/WO₃ (Al₂O₃: 2.2×10^{-2} mg cm⁻²), and (d) Al₂O₃(MOD)/BiVO₄/WO₃ (Al₂O₃: 2.0×10^{-2} mg cm⁻²), calculated by XPS spectra.

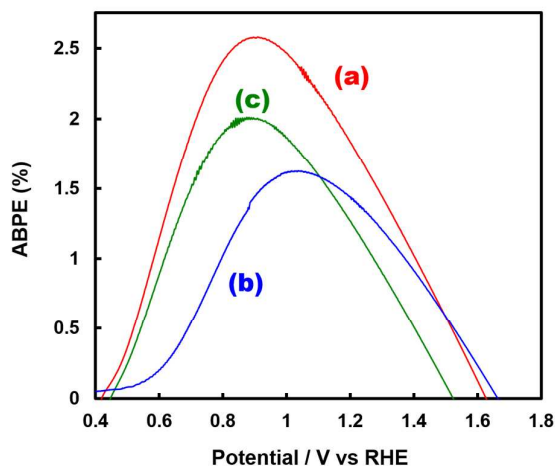


Figure 5. ABPE values for H₂O₂, O₂, and H₂ production after 0.9 C of electric charge was passed in the photoelectrochemical reaction using (a) Al₂O₃(CVD5)/BiVO₄/WO₃ (FE(H₂O₂) = 80%), (b) Al₂O₃(MOD)/BiVO₄/WO₃ (FE(H₂O₂) = 79%), and (c) bare BiVO₄/WO₃ (FE(H₂O₂) = 54%) photoelectrode. FE(H₂O₂) measured in a two-electrode photoelectrochemical cell (Figure S2) and current densities obtained using three-electrode photoelectrochemical cell (Figure 2) were applied to the calculation.

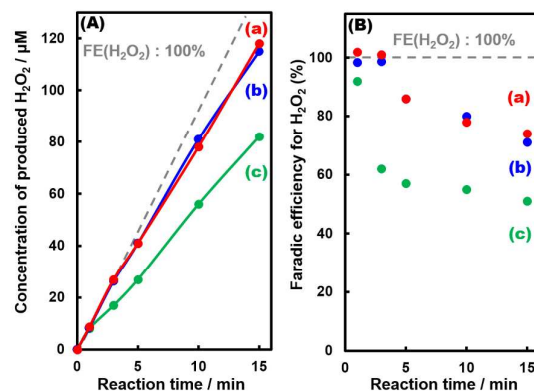


Figure 6. Time courses of (A) concentration of H_2O_2 produced and (B) $\text{FE}(\text{H}_2\text{O}_2)$ in the photoelectrochemical reaction using (a) $\text{Al}_2\text{O}_3(\text{CVD5})/\text{BiVO}_4/\text{WO}_3$, (b) $\text{Al}_2\text{O}_3(\text{MOD})/\text{BiVO}_4/\text{WO}_3$, and (c) bare $\text{BiVO}_4/\text{WO}_3$. Two-electrode photoelectrochemical cell with an photoanode (6 cm^2) and a Pt wire as a cathode electrode was used in a 2.0 M KHCO_3 aqueous solution under CO_2 bubbling and simulated solar irradiation by controlling the stable current of 1.0 mA .

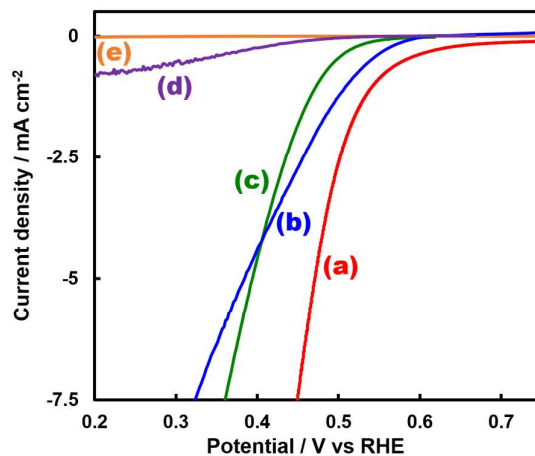


Figure 7. Current density of various cathodes (loading of catalyst: 1.5 mg cm^{-2} ; electrode area: 1 cm^2): (a) WSo_y/GnP, (b) MoSo_y, (c) carbon black (CB), (d) Au wire, and (e) bare CP. Three-electrode cell containing various cathodes (a-d), a Pt wire as an anode and a Ag/AgCl reference electrode was used in 2.0 M KHCO_3 aqueous solution under O_2 bubbling.

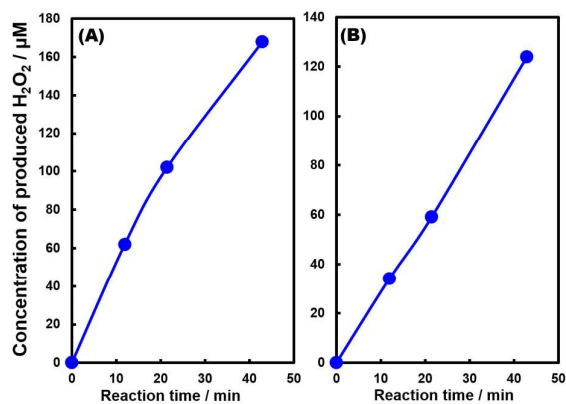
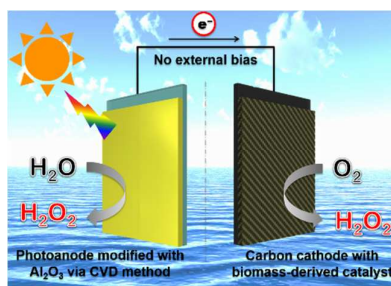


Figure 8. Time course of concentration of H₂O₂ produced on (A) Al₂O₃(CVD5)/BiVO₄/WO₃ photoelectrode (12 cm²) and (B) WSoy/GnP-CP cathode (loading: 1.5 mg cm⁻²) without applying external bias. A two-electrode photoelectrochemical cell with an Al₂O₃(CVD5)/BiVO₄/WO₃ photoelectrode and a WSoy/GnP-CP cathode was used in 2.0 M KHCO₃ aqueous solution under CO₂ bubbling and simulated solar irradiation

Reference

1. A. Fujishima, K. Honda, *Nature*, 1972, **238**, 37.
2. M. Grätzel, *Nature*, 2001, **414**, 338.
3. R. Abe, *J. Photochem. Photobiol. C*, 2010, **11**, 179.
4. G. Hodes, D. Cahen and J. Manassen, *Nature*, 1976, **260**, 312.
5. C. Santato, M. Ulmann and J. Augustynski, *J. Phys. Chem. B*, 2001, **105(5)**, 936.
6. B. Yang, P. R. F. Barnes, Y. Zhang and V. Luca, *Catal. Lett.*, 2007, **118**, 280.
7. K. Sayama, K. Nomura, Z. Zou, R. Abe, Y. Abe and H. Arakawa, *Chem. Commun.*, 2003, **23**, 2908.
8. T. W. Kim, Y. Ping, G. A. Galli and K. S. Choi, *Nature Communications*, 2015, **6**, 8769.
9. J. H. Kennedy and N. Anderman, *J. Electrochem. Soc.*, 1983, **130**, 848.
10. A. Kudo, K. Omori and H. Kato, *J. Am. Chem. Soc.*, 1999, **121**, 11459.
11. I. Dincer and C. Acar, *International Journal of Hydrogen Energy*, 2015, **40**, 11094.
12. K. Ueno and H. Misawa, *NPG Asia Mater.*, 2013, **5**, e61.
13. K. Fuku and K. Sayama, *Chem. Commun.*, 2016, **52**, 5406.
14. K. Fuku, Y. Miyase, Y. Miseki, T. Funaki, T. Gunji and K. Sayama, *Chem. Asian J.*, 2017, **12**, 1111.
15. K. Fuku, Y. Miyase, Y. Miseki, T. Gunji and K. Sayama, *RSC Advances*, 2017, **7**, 47619.
16. X. Shi, S. Siahrostami, G. L. Li, Y. Zhang, P. Chakthranont, F. Studt, T. J. Jaramillo, X. Zheng and J. K. Nørskov, *Nature Communications*, 2017, **8**, 701.
17. Z. Lu, G. Chen, S. Siahrostami, Z. Chen, K. Liu, J. Xie, L. Liao, D. Lin, T. F. Jaramillo and J. K. Nørskov, *Nature Catalysis*, 2018, doi:10.1038/s41929-017-0017-x.
18. Q. Mi, A. Zhanaidarova, B. S. Brunshwig, H. B. Gray and N. S. Lewis, *Energy Environ. Sci.*, 2012, **5**, 5694.
19. K. Fuku, N. Wang, Y. Miseki, T. Funaki and K. Sayama, *ChemSusChem*, 2015, **8**, 1593.
20. S. Iguchi, Y. Miseki, K. Sayama, *Sustainable Energy Fuels*, 2018, **2**, 155.
21. R. Nakamura and Y. Nakato, *J. Am. Chem. Soc.*, 2004, **126**, 1290.
22. R. A. Sheldon and J. Dakka, *Catal. Today*, 1994, **19**, 215.
23. R. Noyori, M. Aoki and K. Sato, *Chem. Commun.*, 2003, 1977.
24. K. Otsuka and I. Yamanaka, *Electrochimica Acta.*, 1990, **35**, 319.
25. D. E. Richardson, H. Yao, K. M. Frank and D. A. Bennet, *J. Am. Chem. Soc.*, 2000, **122**, 1729.

26. R. Saito, Y. Miseki and K. Sayama, *Chem. Commun.*, 2012, **48**, 3833.
27. I. Fujimoto, N. Wang, R. Saito, Y. Miseki T. Gunji and K. Sayama, *Int. J. Hydrogen Energy*, 2014, **39**, 2454.
28. K. Fuku, Y. Miyase, Y. Miseki, T. Gunji and K. Sayama, *Chemistry Select*, 2016, **1**, 5721.
29. S. J. Hong, S. Lee, J. S. Jang and J. S. Lee, *Energy Environ. Sci.*, 2011, **4**, 1781.
30. W. Chen, S. Iyer, S. Iyer, K. Sasaki, C. H. Wang, Y. Zhu, J. T. Muckerman and E. Fujita, *Energy Environ. Sci.*, 2013, **6**, 1818.
31. F. Meng, E. Hu, L. Zhang, K. Sasaki, J. T. Muckerman and E. Fujita, *J. Mater. Chem. A*, 2015, **3**, 18572.
32. K. Sayama, A. Nomura, T. Arai, T. Sugita, R. Abe, M. Yanagida, T. Oi, Y. Iwasaki, Y. Abe and H. Sugihara, *J. Phys. Chem. B*, 2006, **110**, 11352.
33. P. R. Mishra, P. K. Shukla and O. N. Srivastava, *Int. J. Hydrogen Energy*, 2007, **32**, 1680.
34. A. Kaplan, E. Kolin, S. Halevy and A. Bettlheim, *Electrochemistry Communications*, 2015, **60**, 97.

Graphical abstract**Highlight**

The efficient photoelectrochemical H_2O_2 production on both $\text{Al}_2\text{O}_3/\text{BiVO}_4/\text{WO}_3$ photoanode and carbon cathode loaded with bio-mass derived cathode without external bias was demonstrated.